International Research Journal of Engineering and Technology (IRJET) e-ISSN: 2395-0056
Volume: 11 Issue: 06 | Jun 2024 www.irjet.net p-ISSN: 2395-0072

Drone-based Visualization of Radio Signals

Peter Fuhr[1], Elizabeth Piersall[2], Gary Hahn[3], Jason Richards[3]

[1]*Distinguished Scientist, Oak Ridge National Laboratory, Oak Ridge, TN 37831 USA*
[2]*Research Scientist, Oak Ridge National Laboratory, Oak Ridge, TN 37831 USA*
[3]*Technical Professional, Oak Ridge National Laboratory, Oak Ridge, TN 37831 USA*

Abstract - *A system for detecting radio frequency (RF) signals using a set of four software defined radio (SDR) detectors with directional antennas and then displaying them in a visual heatmap manner is described. With the directional antennas pointing in differing (but slightly overlapping) directions, a 1 MHz bandwidth frequency band within the 902-928 MHz spectrum is chosen for analysis. The outputs from the SDRs are measured and analyzed from which an intensity/color variable structured light pattern is generated. The four light patterns, one for each directional SDR, are arranged in a four-quadrant pattern and overlaid by a visual image of the RF measurement location. The system may be mounted on a drone thereby providing RF signal direction finding from an aerial platform. A description of this design, which is constructed based on a combination of optical and RF techniques and technologies is described. The net result being an Enhanced Reality (ER) view of signals in selected radio frequencies with integration within the Autonomous Intelligence Measurement Sensors and Systems (AIMS) project.*

Key Words: software defined radio, drones, sensors, structured light

1.INTRODUCTION

Radio frequency (RF) signals may be converted into visible optical representation through the use of a combination of directional antennae, RF detectors, Software Defined Radios (SDRs) and mathematical signal processing. Directionality is achieved in the following manner: each directional antenna arranged in a matrix/array subtends an angle that is identical to its array "neighbors[1]" but each is pointing in slightly different directions due to the (machined/printed) antenna mounts. Algorithmic processing allows for varying the tunable SDRs thereby having the capability to scan radio frequencies. In addition, the microprocessor acquires the signal strength readings from each SDR, then records those values into an NxN matrix. The radio signal level of each matrix element is mapped to a signal level that is used to set the intensity and wavelength of an array of LEDs (or similar light source).

Furthermore, using this array technique, each RF detector system – comprised of the aforementioned directional antenna and connected SDR - subtends a specific angular field-of-view thereby allowing the spatial extent of the RF wavefront's intensity to be measured. As illustrated in Figure 1, a microprocessor is connected to the output of the detector array allowing a numeric value for each detector measured intensity to be obtained. The detection frequency range is variable through the use of the SDRs (one SDR per directional antenna).

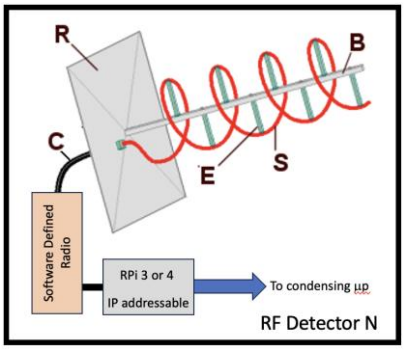

Fig-1. Directional antenna, software defined radio (SDR) and microprocessor are the principal components of the radio detection portion of the device.

Determination of the direction to the RF signal source utilizes centroid detection mathematics associated with optical quadrant detectors [1-3], Figure 2.

[1] Identical RF antennas are used – therefore with identical fields-of-view (radiation pattern). Each antenna is pointing in a slightly different direction than the others.

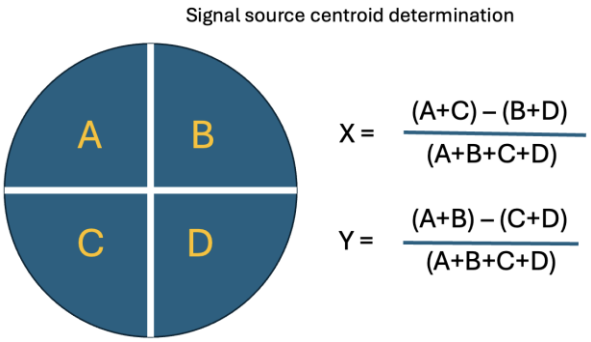

Fig-2. Optical quadrant detection centroid determination.

Figure 3 is meant to illustrate how each antenna has an identical "field of view" but is pointing in a unique direction. In addition, an interfaced camera has the center of its field of view aligned with the center (intersection point) of the RF antennas. This arrangement provides an enhanced reality view of the RF measurements with a view as to where the system is "looking".

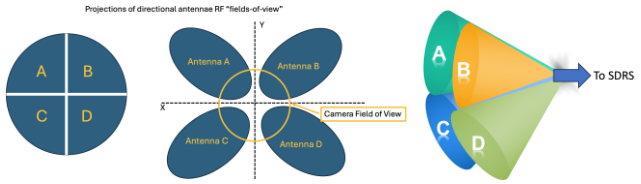

Fig-3. Directional antennae and companion visible camera fields of view.

2. HARDWARE

The proof-of-principle system utilized four directional antennas and their associated RTL-SDR V3s. Initially, each SDR was interfaced to a Raspberry Pi in a one-to-one correspondence, Figure 4.a. Initial testing incorporated directional antennas that were tuned outside of the SDRs' RF tuning range (500 kHz - 1.7 GHz). The Yagi antennas in Figure 4 provided 10dB gain across the 2.355 - 2.6 GHz frequency range. Placement of the antennas into a Styrofoam disc, Figure 4.b, allowed for prototype-level determination of the antennae mechanical angles to achieve the slight radiation/detection pattern overlap shown in Figure 3.

(a) (b)

Fig-4. (a) Initial hardware configuration. (b) Directional antennas mounted in a Styrofoam disc.

Initial system trials indicated that the software used for the SDR signal processing was relatively computationally "light". Therefore, the hardware configuration was modified with only one RPi being used[2], Figure 5. Note that the power requirements for each SDR, 270-280mA at 5V, necessitated use of a four-port powered USB switch and a single RPi (350mA, 1.9W). (again, Figure 5).

Fig-5. Optimized hardware configuration: RTL-SDR into powered USB Switch into Raspberry Pi3.

3. SOFTWARE

The output from the set of RF detectors is read using the rtl_power utility that comes with the librtlsdr library. An RMS value is calculated from the FFT measurements provided from rtl_power each second. Centroid determination is performed using each detector/quadrant's RMS value in the equation shown in Figure 2. The RMS is then normalized to the range 0 to 1 to map the signal strength to a heat map palette color. The RPi then sequentially steps through the RF signal array (in this case

[2] This reduction in number of RPi's had the associated benefit of reducing the power requirements as well as packaging of the components both of which impacted (simplified) the "package" mounted on the drone.

2x2) mapping the normalized RMS detector signal level to the associated heatmap color, Figure 6. The resultant optical field represents the signal strength of the RF signal which is a visual representation of the invisible RF field. Figure 7 presents a quadrant RF heatmap overlaid onto a visible camera image.

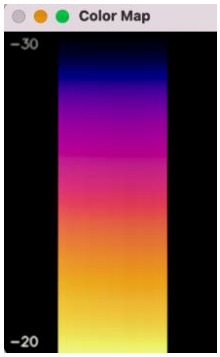

Fig-6. Heat map color palette (signal strength represented here as a logarithmic signal range of -20 to -30 dBm).

An alternative method is to use the software application gqrx 2.17. This was used to configure and retrieve measurements from the SDRs. While gqrx has numerous visualization options, only its analysis capabilities were used. Specifically, a Fast Fourier Transform (FFT) of 16384 data points with a residual bandwidth of 109.9 Hz with a Hamming window was used for calculation of the maximum power in the frequency range of interest (in this case 906-907 MHz).

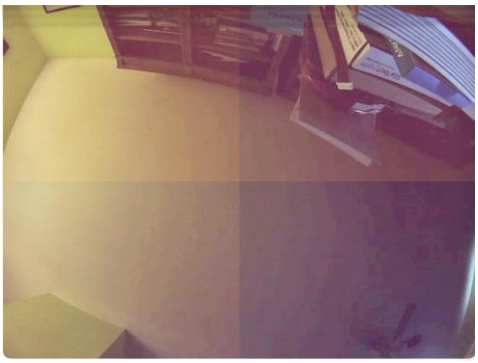

Fig-7. Quadrant heatmap.

In this configuration, the USB visual camera was attached to the RPi with image streaming via RTSP to the application Shinobi using gstreamer. While seemingly complex, this overall multi-application software system had minimal impact on the RPi's CPU/memory. The result is an image of the received RF signal strength with the frequency being scanned variable.

A standalone Shinobi network video recorder (NVR) server is used to provide for configuration and use of the enhanced reality video image (visible plus quadrant RF heatmaps). For ease of use, Shinobi handles the different "monitors" for each of the camera streams. As an NVR, the application can also perform functions such as automatically recording video clips, motion detection, snapshots, etc. One issue encountered with this software arrangement is that there is a few milliseconds delay on top of whatever latency that is associated with the original camera stream if you are watching "live" through Shinobi. Note that the RF RPi outputs two streams. One is the USB visual camera RTSP stream. The heatmap is used as an overlay on this stream to generate a new MJPEG stream.[3] An alternatively to watching the streams via Shinobi is to view in a browser or VLC therefore having slightly less delay. The application process is:

RF Pi -> MJPEG stream (heatmap + visual camera) -> Shinobi
-> RTSP stream (visual USB camera only)

Relying on IP addressing and assigned ports allows for accessing the camera streams in the following manner:
Cameras RPi (hostname "rpi-cameras"):
rtsp://<IP_Address>:8554:/visual
rtsp://<IP_Address>:8554:/thermal
rtsp://<IP_Address>:8554:/uv

RF RPi (hostname "rpi-rf"):
http://<IP_Address>:8083

Applications rely on username+password authentication for a modicum of cybersecurity.

4. DRONE-BASED SYSTEM

Having demonstrated the visualization of RF system using a static, stationary system, the next step was to deploy the system elements on a drone (mobile platform). The principal elements used in the drone mounted, but stationary, 2x2 proof of concept system configuration were:
(1) RTL-SDRs tuned to a 1 MHz "range", 906-907 Hz (tunable frequency range: 500kHz - 1766 MHz);
(2) antennae frequency range: 2335-2600 MHz with an antenna gain: 10.5dB (typical value).
The mismatch between scanned frequency and the antenna frequency passband was noted but did not affect the system operations. The system shown in Figure 8 is based on a HolyBro X500 V2 (kit) drone. The antennas used were for verification of the radiation patterns as well as drone flight stability testing with the antenna mounting arrangement.

[3] Development of an RTSP interface and access method is underway. This should lessen or eliminate the latency and delay issues.

Fig-8. Drone mounted system.

With those tests completed, TAOGLAS antennas[4] - optimized for the 906-907 MHz frequency band - along with the four RTL-SDRs and system batteries were attached to the drone, Figure 9.

Fig-9. Configured drone with SDRs and associated components.

Operation of the system necessitated a Wi-Fi network providing wireless coverage[5] within which the drone flew. With overlaid heatmap visualization formed using the drone-mounted RPi (edge processing), a ground-based laptop accessed the RPi via IP addressing. Through this network configuration the laptop displayed the measurements in real-time as the drone flew around the test area, Figure 10.

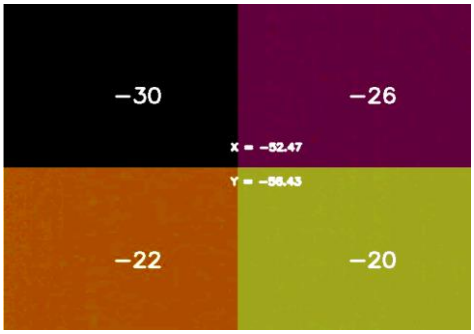

Fig-10. RF signal strength levels for each zone.

Varying RF signal strength in the four antennas' radiation pattern (acceptance solid angle) and use of centroid determination (equations in Figure 2) results in the differing colors per zone. The centroid locations (relative to the 2x2 detection "size") are also displayed. Note that the signal strengths are in decibels relative to 1 mWatt. Therefore, zone D, with a signal strength of -20 dBm is stronger than zone A (-30 dBm).

5. Summary

A system to provide aerial measurements/scans of RF signal sources has been developed. The RF signal levels are processed resulting in a graphical display of the signal strength as colors. This colorful heatmap is overlaid onto a camera stream to provide a view of what area is being scanned. Performance verification took place within a laboratory-based environment. The measurement system was then integrated onto a drone platform, see Figure 11, performance validated with other AIMS systems, as well as in-field at an electric utility's substation.

Fig-11. The AIMS SDR RF measurement and visualization system, drone mounted.

[4] The TAOGLAS antennas are black and rectangular in shape in Figure 9.

[5] similar to an umbrella

5. REFERENCES

[1] *Y. Zheng, H. Chen and Z. Zhou, "Angle measurement of objects outside the linear field of view of a strapdown semi-active laser seeker", Sensors 2018, 18, 1673; doi:10.3390/s18061673*

[2] *L. Zhang, Y. Yang, W. Xia,; X. Zhu, W. Chen,; Y. Lu, "Linearity of quadrant avalanche photodiode in laser tracking system". Chin. Opt. Lett. 2009, 7, 728–731.*

[3] *Chen, M.; Yang, Y.; Jia, X.; Gao, H. "Investigation of positioning algorithm and method for increasing the*

[4] *linear measurement range for four-quadrant detector". Optik Int. J. Light Electr. Opt. 2013, 124, 6806–6809.*